# Atmospheric Chemistry of a Model Biodiesel Fuel, $CH_3C(O)O(CH_2)_2OC(O)CH_3$: Kinetics, Mechanisms, and Products of Cl Atom and OH Radical Initiated Oxidation in the Presence and Absence of $NO_x$

**M. D. Hurley,* J. C. Ball, and T. J. Wallington**

*Physical & Environmental Sciences Department, Ford Motor Company, Mail Drop SRL-3083, Dearborn, Michigan 48121*

**A. Toft**

*Department of Chemistry, University of Southern Denmark, Campusvej 55, DK-5230 Odense M, Denmark*

**O. J. Nielsen**

*Department of Chemistry, University of Copenhagen, Universitetsparken 5, DK-2100 Copenhagen, Denmark*

**S. Bertman and M. Perkovic†**

*Department of Chemistry, Western Michigan University, Kalamazoo, Michigan 49008*

*Received: October 13, 2006; In Final Form: December 20, 2006*

Relative rate techniques were used to study the kinetics of the reactions of Cl atoms and OH radicals with ethylene glycol diacetate, $CH_3C(O)O(CH_2)_2OC(O)CH_3$, in 700 Torr of $N_2/O_2$ diluent at 296 K. The rate constants measured were $k(Cl + CH_3C(O)O(CH_2)_2OC(O)CH_3) = (5.7 \pm 1.1) \times 10^{-12}$ and $k(OH + CH_3C(O)O(CH_2)_2OC(O)CH_3) = (2.36 \pm 0.34) \times 10^{-12}$ cm$^3$ molecule$^{-1}$ s$^{-1}$. Product studies of the Cl atom initiated oxidation of ethylene glycol diacetate *in the absence of NO* in 700 Torr of $O_2/N_2$ diluent at 296 K show the primary products to be $CH_3C(O)OC(O)CH_2OC(O)CH_3$, $CH_3C(O)OC(O)H$, and $CH_3C(O)OH$. Product studies of the Cl atom initiated oxidation of ethylene glycol diacetate *in the presence of NO* in 700 Torr of $O_2/N_2$ diluent at 296 K show the primary products to be $CH_3C(O)OC(O)H$ and $CH_3C(O)OH$. The $CH_3C(O)OCH_2O\bullet$ radical is formed during the Cl atom initiated oxidation of ethylene glycol diacetate, and two loss mechanisms were identified: reaction with $O_2$ to give $CH_3C(O)OC(O)H$ and α-ester rearrangement to give $CH_3C(O)OH$ and HC(O) radicals. The reaction of $CH_3C(O)OCH_2O_2\bullet$ with NO gives chemically activated $CH_3C(O)OCH_2O\bullet$ radicals which are more likely to undergo decomposition via the α-ester rearrangement than $CH_3C(O)OCH_2O\bullet$ radicals produced in the peroxy radical self-reaction.

## 1. Introduction

Energy security and climate change concerns have prompted increased interest in alternative transportation fuels derived from biogenic sources.[1−3] The principal biofuels under consideration are methyl esters of long chain fatty acids (e.g., $CH_3(CH_2)_7CH{=}CH(CH_2)_7C(O)OCH_3$ from oleic acid and $C_{15}H_{31}C(O)OCH_3$ from palmitic acid) for blending in diesel fuel and alcohols (e.g., $C_2H_5OH$, $C_3H_7OH$, and $C_4H_9OH$) for blending in gasoline. Biodiesel has an energy density which is similar to that of petroleum diesel and so provides similar fuel economy. Biodiesel is made via a relatively simple transesterification process from triglycerides.

During biodiesel production, glycerine ($CH_2OHCH(OH)CH_2OH$, propane-1,2,3-triol) is formed in significant quantities as a coproduct. One of the technical hurdles facing the biodiesel industry is finding commercially attractive uses for glycerine. One possible use for this material is to convert it into a compound for blending with diesel fuel. Glycerine is not a viable blending component because of its low solubility in hydrocarbons and high affinity for water. However, glycerine can be transformed into compounds with more suitable blending properties. For example, acylation using acetic acid, propionic acid, or longer chain acids provides molecules which are more soluble in hydrocarbon solvents like diesel fuel and less soluble in water. Prior to the use of such acylated glyercine derivatives, information on their atmospheric chemistry is required. In this study we investigate the atmospheric fate of ethylene glycol diacetate, $CH_3C(O)O(CH_2)_2OC(O)CH_3$, as a model compound for such acylated glycerine molecules. Ethylene glycol diacetate was chosen as a model because its vapor pressure is greater than, but its chemistry is expected to be similar to, the analogous acylated glycerine derivatives.

## 2. Experimental Section

The experiments were performed in a 140-L Pyrex reactor interfaced to a Mattson Sirus 100 FTIR spectrometer. The reactor was surrounded by 22 fluorescent blacklamps (GE F15T8-BL) which were used to photochemically initiate the experiments. Chlorine atoms were produced by photolysis of molecular chlorine.

$$Cl_2 + h\nu \rightarrow Cl + Cl \quad (1)$$

* Corresponding author e-mail: mhurley3@ford.com.
† Deceased.

10.1021/jp0667341 CCC: $37.00 
Published on Web 03/15/2007

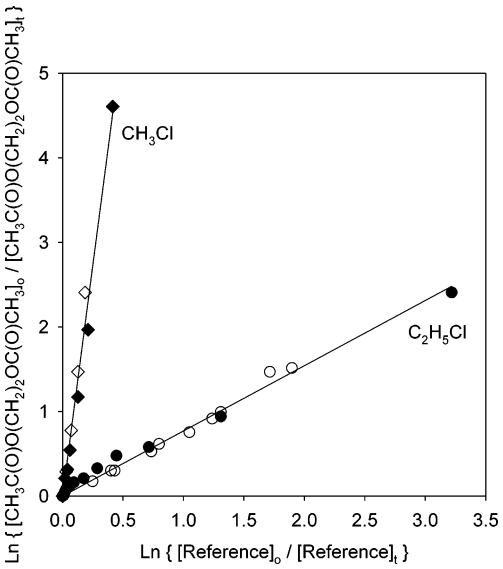


**Figure 1.** Decay of $CH_3C(O)O(CH_2)_2OC(O)CH_3$ versus $C_2H_5Cl$ (circles) and $CH_3Cl$ (diamonds) in the presence of Cl atoms in 700 Torr of either air (filled symbols) or $N_2$ (open symbols) at 296 ± 1 K.

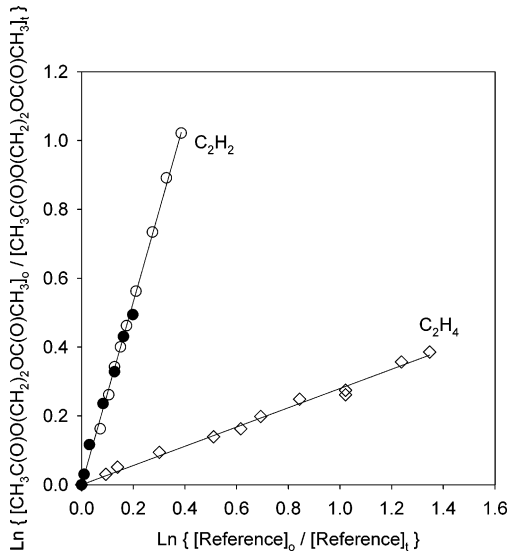


**Figure 2.** Decay of $CH_3C(O)O(CH_2)_2OC(O)CH_3$ versus $C_2H_4$ (diamonds) and $C_2H_2$ (circles) in the presence of OH radicals in 700 Torr of air with (closed symbols) and without (open symbols) added NO at 296 ± 1 K.

OH radicals were produced by photolysis of $CH_3ONO$ in the presence of NO in air.

$$CH_3ONO + h\nu \rightarrow CH_3O\bullet + NO \quad (2)$$

$$CH_3O\bullet + O_2 \rightarrow HO_2 + HCHO \quad (3)$$

$$HO_2 + NO \rightarrow OH + NO_2 \quad (4)$$

Relative rate techniques were used to measure the rate constant of interest relative to a reference reaction whose rate constant has been established previously. The relative rate method is a well-established technique for measuring the reactivity of Cl atoms and OH radicals with organic compounds.[4] Kinetic data are derived by monitoring the loss of $CH_3C(O)O(CH_2)_2OC(O)CH_3$ relative to one or more reference compounds. The decays of $CH_3C(O)O(CH_2)_2OC(O)CH_3$ and the reference are then plotted using the expression

$$\mathrm{Ln}\left(\frac{[\text{reactant}]_0}{[\text{reactant}]_t}\right) = \frac{k_{\text{reactant}}}{k_{\text{reference}}} \times \mathrm{Ln}\left(\frac{[\text{reference}]_0}{[\text{reference}]_t}\right) \quad \text{(I)}$$

where $[\text{reactant}]_0$, $[\text{reactant}]_t$, $[\text{reference}]_0$, and $[\text{reference}]_t$ are the concentrations of $CH_3C(O)O(CH_2)_2OC(O)CH_3$ and the reference compound at times "0" and "*t*", and $k_{\text{reactant}}$ and $k_{\text{reference}}$ are the rate constants for reactions of Cl atoms or OH radicals with the $CH_3C(O)O(CH_2)_2OC(O)CH_3$ and the reference compound. Plots of $\mathrm{Ln}([\text{reactant}]_0/[\text{reactant}]_t)$ versus $\mathrm{Ln}([\text{reference}]_0/[\text{reference}]_t)$ should be linear, pass through the origin, and have a slope of $k_{\text{reactant}}/k_{\text{reference}}$.

$CH_3ONO$ was synthesized by the dropwise addition of concentrated sulfuric acid to a saturated solution of $NaNO_2$ in methanol.[5] Acetoxyacetic acetic anhydride, $CH_3C(O)OC(O)CH_2OC(O)CH_3$, was prepared from acetoxyacetyl chloride (Aldrich) and sodium acetate in tetrahydrofuran as described by Schijf and Stevens.[6] Acetoxyacetic acetic anhydride was purified by repeated bulb-to-bulb vacuum transfers. The sample of acetoxyacetic acetic anhydride contained acetic anhydride which could not be removed, possibly due to the formation of an azeotropic mixture. The presence of the acetic anhydride impurity, together with the low vapor pressure of acetoxyacetic acetic anhydride, prevented an absolute calibration of the acetoxyacetic acetic anhydride reference spectrum. Other reagents were obtained from commercial sources. Experiments were conducted in 700 Torr total pressure of $O_2/N_2$ diluent at 296 ± 1 K. Concentrations of reactants and products were monitored by FTIR spectroscopy. IR spectra were derived from 32 coadded interferograms with a spectral resolution of 0.25 $cm^{-1}$ and an analytical path length of 27 m.

In smog chamber experiments it is important to check for the unwanted loss of reactants and products via photolysis, dark chemistry, and heterogeneous reactions. Control experiments were performed in which (i) mixtures of reactants (except $Cl_2$) were subjected to UV irradiation for 10−20 min and (ii) product mixtures obtained after the UV irradiation of reactant mixtures were allowed to stand in the dark in the chamber for 20 min. There was no observable loss of reactants or products, suggesting that photolysis, dark chemistry, and heterogeneous reactions are not significant complications in the present work. Unless stated otherwise, quoted uncertainties are two standard deviations from least-squares regressions.

## 3. Results

**3.1. Relative Rate Study of $k(Cl + CH_3C(O)O(CH_2)_2OC(O)CH_3)$.** The kinetics of reaction 5 were measured relative to those of reactions 6 and 7:

$$Cl + CH_3C(O)O(CH_2)_2OC(O)CH_3 \rightarrow \text{products} \quad (5)$$

$$Cl + CH_3Cl \rightarrow \text{products} \quad (6)$$

$$Cl + C_2H_5Cl \rightarrow \text{products} \quad (7)$$

Reaction mixtures consisted of 1.9−2.6 mTorr of $CH_3C(O)O(CH_2)_2OC(O)CH_3$, 88−103 mTorr $Cl_2$, and 14.7−30.1 mTorr of either $C_2H_5Cl$ or $CH_3Cl$ in a total of 700 Torr air or $N_2$. The observed loss of $CH_3C(O)O(CH_2)_2OC(O)CH_3$ versus those of the reference compounds is plotted in Figure 1. Linear least-squares analysis of the data in Figure 1 gives $k_5/k_6 = 10.9 \pm 1.1$ and $k_5/k_7 = 0.77 \pm 0.08$. Using $k_6 = 4.8 \times 10^{-13}$ [7] and $k_7 = 8.04 \times 10^{-12}$ [8] gives $k_5 = (5.2 \pm 0.5) \times 10^{-12}$ and $(6.2 \pm 0.6) \times 10^{-12}$ $cm^3$ $molecule^{-1}$ $s^{-1}$. Indistinguishable values of $k_5$ are obtained using the two different references. We choose

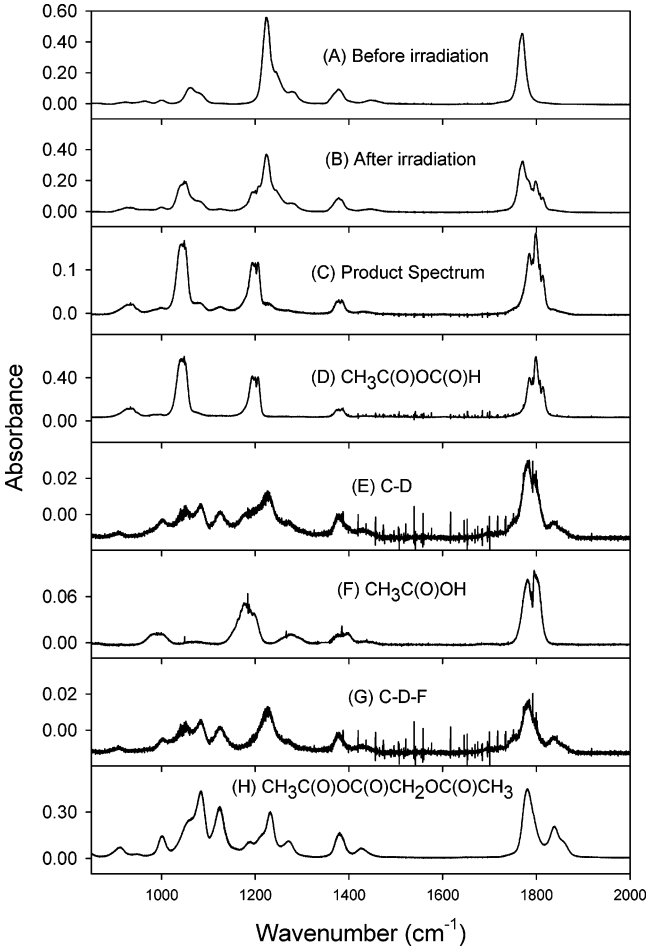


**Figure 3.** IR spectra obtained before (A) and after (B) a 15 s irradiation of 3.9 mTorr of $CH_3C(O)O(CH_2)_2OC(O)CH_3$ and 92 mTorr of $Cl_2$ in 700 Torr air. (C) shows the IR product spectrum. (E) shows the product spectrum after the subtraction of features due to $CH_3C(O)OC(O)H$. (G) shows the product spectrum after the subtraction of features due to $CH_3C(O)OC(O)H$ and $CH_3C(O)OH$.

to cite a final value which is the average of the individual determinations together with error limits which encompass the extremes of the determinations; therefore, $k_5 = (5.7 \pm 1.1) \times 10^{-12}$ cm$^3$ molecule$^{-1}$ s$^{-1}$.

**3.2. Relative Rate Study of $k$(OH + $CH_3C(O)O(CH_2)_2OC(O)CH_3$).** The kinetics of reaction 8 were measured relative to reactions 9 and 10:

$$OH + CH_3C(O)O(CH_2)_2OC(O)CH_3 \rightarrow \text{products} \quad (8)$$

$$OH + C_2H_4 \rightarrow \text{products} \quad (9)$$

$$OH + C_2H_2 \rightarrow \text{products} \quad (10)$$

Initial reaction mixtures consisted of 1.8−2.5 mTorr of $CH_3C(O)O(CH_2)_2OC(O)CH_3$, 0−19 mTorr of NO, 95−102 mTorr $CH_3ONO$, and 7.2−11.5 mTorr of either $C_2H_4$ or $C_2H_2$ in 700 Torr total pressure of air diluent. Figure 2 shows the loss of $CH_3C(O)O(CH_2)_2OC(O)CH_3$ plotted versus loss of the reference compounds. Linear least-squares analysis gives $k_8/k_9 = 0.28 \pm 0.03$ and $k_8/k_{10} = 2.7 \pm 0.3$. Using $k_9 = 8.7 \times 10^{-12}$ [9] and $k_{10} = 8.45 \times 10^{-13}$ [10] we derive $k_8 = (2.44 \pm 0.26) \times 10^{-12}$ and $(2.28 \pm 0.26) \times 10^{-12}$. Indistinguishable values of $k_8$ are obtained using the two different references. We choose to cite a final value which is the average of the individual determinations together with error limits which encompass the extremes of the determinations; therefore, $k_8 = (2.36 \pm 0.34) \times 10^{-12}$ cm$^3$ molecule$^{-1}$ s$^{-1}$. While there have been no previous measurements of $k_8$, O'Donnell et al.[11] have reported rate coefficients for reactions of OH radicals with a series of related alkoxy esters. They report $k(OH+CH_3C(O)O(CH_2)_2OCH_3) = (7.83 \pm 0.31) \times 10^{-12}$ and $k(OH+CH_3C(O)O(CH_2)_2OC_2H_5) = (1.21 \pm 0.29) \times 10^{-11}$ cm$^3$ molecule$^{-1}$ s$^{-1}$ at 298 K. Consistent with the available data concerning the reactivity of ethers and esters, $CH_3C(O)O(CH_2)_2OC(O)CH_3$ is approximately 3 times less reactive than $CH_3C(O)O(CH_2)_2OCH_3$ reflecting the fact that $-OCH_3$ is more activating than the $-OC(O)CH_3$ group.

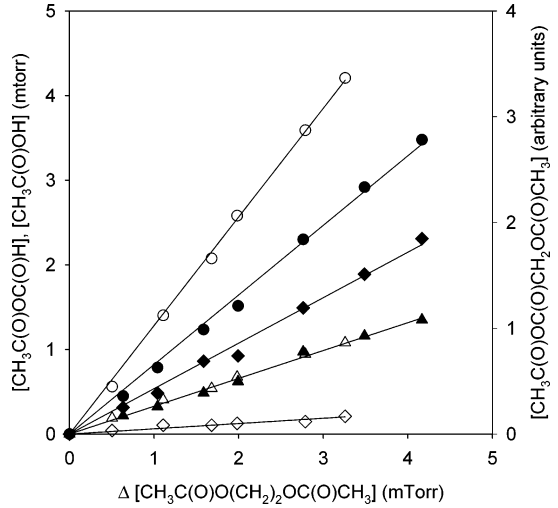


**Figure 4.** Formation of $CH_3C(O)OC(O)H$ (circles), $CH_3C(O)OH$ (diamonds), and $CH_3C(O)OC(O)CH_2OC(O)CH_3$ (triangles) versus the loss of $CH_3C(O)O(CH_2)_2OC(O)CH_3$ following the UV irradiation of mixtures of $CH_3C(O)O(CH_2)_2OC(O)CH_3$ and $Cl_2$ in the presence of either 5 (closed symbols) or 700 Torr $O_2$ (open symbols) in 700 Torr total pressure made up with $N_2$ as appropriate. The lines are least-squares linear fits to the data.

**3.3. Structure−Activity Relationships.** The kinetic results can be compared with the rate coefficients predicted using the structure−activity relationship (SAR) approach developed by Atkinson and co-workers.[12−14] The SAR method provides a means of calculating the rate of reaction of the OH radical with a large number of organic compounds. Calculation of the H-atom abstraction rate from C−H bonds is based on the estimated $-CH_3$, $-CH_2-$, and $>CH-$ group rate constants, where the group rate constant is influenced by the nature of the α substituent groups. Agreement with experimental values is generally good, except in cases where long-range effects require consideration of $\beta$ substituent groups. Using the group rate constants and substituent factors recommended by Kwok and Atkinson,[13] the rate constant for reaction 8 is calculated to be $k_8(SAR) = 3.9 \times 10^{-12}$ cm$^3$ molecule$^{-1}$ s$^{-1}$. Mellouki et al.[15] reviewed the kinetics and mechanisms of the oxidation of oxygenated organic compounds and have proposed group rate constants for ester $CH_x$ ($x$ = 1,2,3) groups that depend on whether the $CH_x$ group is on the acyl or alkoxy group of the ester and whether the $CH_x$ group is in the α, $\beta$, $\gamma$, or $\delta$ position. Using the appropriate group rate constants, this approach gives a value of $k_8 = 3.0 \times 10^{-12}$ cm$^3$ molecule$^{-1}$ s$^{-1}$. Using the group rate constants from Mellouki et al.[15] we conclude that 7% of OH atom attack occurs at the terminal $-CH_3$ group, while 93% of OH atom attack occurs at the bridging $-CH_2-$ groups. Mellouki et al.[15] also discuss the reactivity of bridging $-CH_2-$ groups in difunctional oxygenated compounds. They cite examples where the reactivity of the bridging $-CH_2-$ groups is the same as expected from α substituents and examples where

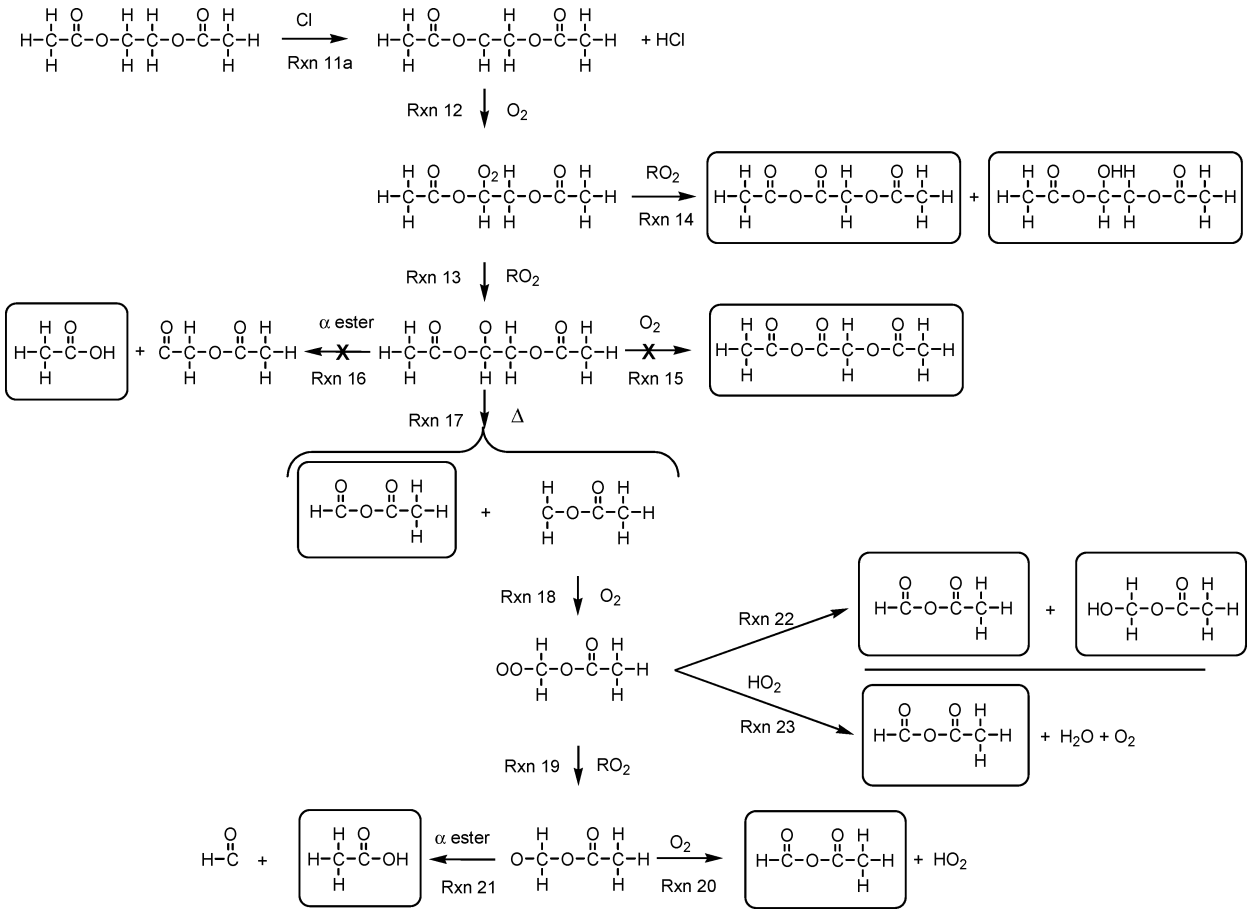


**Figure 5.** Diagram of the chlorine initiated oxidation of ethylene glycol diacetate in the absence of NO.

the reactivity is enhanced, suggesting the effect of long-range activation. The experimental value determined in this work, $k_8 = (2.36 \pm 0.34) \times 10^{-12}$ cm$^3$ molecule$^{-1}$ s$^{-1}$, is consistent with the SAR estimates of both Kwok and Atkinson[13] and Mellouki et al.[15] Finally, Notario et al.[16] extended the SAR approach to the reaction of Cl atoms with a series of esters. Using the modified SAR approach of Notario et al.[16] gives $k_5$(SAR) $= 5.0 \times 10^{-12}$ cm$^3$ molecule$^{-1}$ s$^{-1}$, which is consistent with the experimental value determined in this work, $k_5 = (5.7 \pm 1.1) \times 10^{-12}$ cm$^3$ molecule$^{-1}$ s$^{-1}$.

**3.4. Products of the Cl Atom Initiated Oxidation of $CH_3C(O)O(CH_2)_2OC(O)CH_3$ in the Absence of NO.** The Cl atom initiated oxidation of ethylene glycol diacetate in the absence of NO was investigated by irradiating mixtures containing 2−5 mTorr $CH_3C(O)O(CH_2)_2OC(O)CH_3$ and 86−100 mTorr $Cl_2$ in 700 Torr of $O_2/N_2$ diluent. Reaction mixtures were subjected to 5−7 successive irradiations of 5−30 s duration. Figure 3 shows spectra acquired before (A) and after (B) a 15 s irradiation of 4.1 mTorr $CH_3C(O)O(CH_2)_2OC(O)CH_3$ and 91.7 mTorr $Cl_2$ in 700 Torr of air. The consumption of $CH_3C(O)O(CH_2)_2OC(O)CH_3$ was 41%. Panel (C) shows the product spectrum obtained by subtracting $CH_3C(O)O(CH_2)_2OC(O)CH_3$ features from panel B. Comparison of panel (C) with the reference spectrum in panel (D) shows that acetic formic anhydride, $CH_3C(O)OC(O)H$, is an important product. Panel (E) shows the result of subtracting $CH_3C(O)OC(O)H$ features from panel (C). Comparison of panel (E) with the reference spectrum in panel (F) shows that acetic acid, $CH_3C(O)OH$, is a product. Panel (G) is the result of subtracting $CH_3C(O)OH$ features from panel (E). Comparison of panel (G) with the reference spectrum in panel (H) shows that $CH_3C(O)OC(O)CH_2OC(O)CH_3$ is a product. Figure 4 shows the formation of products versus the loss of $CH_3C(O)O(CH_2)_2OC(O)CH_3$ for experiments in the presence of either 5 or 700 Torr of $O_2$ at 700 Torr total pressure made up with $N_2$ as appropriate. The linearity of the data suggests that secondary loss or formation of these products is not important under these conditions. The yields of $CH_3C(O)OC(O)H$ and $CH_3C(O)OH$ clearly depend on the $O_2$ concentration, while the yield of $CH_3C(O)OC(O)CH_2OC(O)CH_3$ is independent of $O_2$ concentration.

A diagram of the reaction pathways for the Cl atom initiated oxidation of ethylene glycol diacetate in the absence of $NO_x$ is given in Figure 5. Reaction of $CH_3C(O)OCH_2CH_2OC(O)CH_3$ with Cl atoms can occur via two channels.

$$CH_3C(O)OCH_2CH_2OC(O)CH_3 + Cl \rightarrow CH_3C(O)OC\bullet HCH_2OC(O)CH_3 + HCl \quad (11a)$$

$$CH_3C(O)OCH_2CH_2OC(O)CH_3 + Cl \rightarrow \bullet CH_2C(O)OCH_2CH_2OC(O)CH_3 + HCl \quad (11b)$$

We have no direct measure of the relative importance of the two channels; however, in studies of the Cl and OH initiated oxidation of acetates,[17−20] H atom abstraction from the $CH_3C(O)$ group was found to be of minor importance. Reaction 11a is expected to be the dominant channel, and the observed products are consistent with this assumption. Reaction 11a followed by reaction with $O_2$ results in the formation of alkyl peroxy radicals.

$$CH_3C(O)OC(\bullet)HCH_2OC(O)CH_3 + O_2 \rightarrow CH_3C(O)OCHOO(\bullet)CH_2OC(O)CH_3 \quad (12)$$

In the absence of NO, reaction of $CH_3C(O)OCHOO•CH_2OC(O)CH_3$ with other peroxy radicals results in the formation of alkoxy radicals

$$CH_3C(O)OCHOO•CH_2OC(O)CH_3 + ROO• \rightarrow CH_3C(O)OCHO•CH_2OC(O)CH_3 + RO• + O_2 \quad (13)$$

Self-reaction of $CH_3C(O)OCHOO•CH_2OC(O)CH_3$ radicals to give molecular products is also a possibility.

$$2\,CH_3C(O)OCHOO•CH_2OC(O)CH_3 \rightarrow CH_3C(O)OC(O)CH_2OC(O)CH_3 + CH_3C(O)OCHOHCH_2OC(O)CH_3 \quad (14)$$

The alkoxy radicals formed in reaction 13 can react with $O_2$ to form acetoxyacetic acetic anhydride and $HO_2$.

$$CH_3C(O)OCHO•CH_2OC(O)CH_3 + O_2 \rightarrow CH_3C(O)OC(O)CH_2OC(O)CH_3 + HO_2 \quad (15)$$

Tuazon et al.[17] first reported, and others[18−20] have confirmed, that alkoxy radicals of the form RC(O)OCHO•R′ can undergo a rapid rearrangement and decomposition (α-ester rearrangement) to form RC(O)OH and R′CO•.

$$CH_3C(O)OCHO•CH_2OC(O)CH_3 \rightarrow CH_3C(O)OH + •OCCH_2OC(O)CH_3 \quad (16)$$

The alkoxy radicals formed in reaction 13 can also decompose via C−C bond cleavage.

$$CH_3C(O)OCHO•CH_2OC(O)CH_3 \rightarrow CH_3C(O)OC(O)H + •CH_2OC(O)CH_3 \quad (17)$$

The fate of $CH_3C(O)OC•H_2$ is discussed in detail in a paper on the atmospheric oxidation mechanism of methyl acetate by Christensen et al.[18] It was concluded that $CH_3C(O)OC•H_2$ radicals add $O_2$ and then react with other $RO_2•$ radicals to form $CH_3C(O)OCH_2O•$ radicals.

$$CH_3C(O)OC•H_2 + O_2 \rightarrow CH_3C(O)OCH_2OO• \quad (18)$$

$$CH_3C(O)OCH_2OO• + RO_2 \rightarrow CH_3C(O)OCH_2O• \quad (19)$$

There are two competing loss mechanisms for $CH_3C(O)OCH_2O•$ radicals: reaction with $O_2$ and α-ester rearrangement.

$$CH_3C(O)OCH_2O• + O_2 \rightarrow CH_3C(O)OC(O)H + HO_2• \quad (20)$$

$$CH_3C(O)OCH_2O• \rightarrow CH_3C(O)OH + HCO• \quad (21)$$

Yields of $CH_3C(O)OC(O)H$ and $CH_3C(O)OH$ observed from the Cl initiated oxidation of $CH_3C(O)OCH_2CH_2OC(O)CH_3$ in the absence of NO are shown in Figure 6 as a function of $[O_2]$. The yield of $CH_3C(O)OC(O)H$ increases, while the yield of $CH_3C(O)OH$ decreases with increasing oxygen concentration. The yield of $CH_3C(O)OC(O)CH_2OC(O)CH_3$ is independent of oxygen concentration. The simplest explanation for these results is that $CH_3C(O)OCH_2CH_2OC(O)CH_3$ reacts with Cl in the presence of $O_2$ to form the alkyl peroxy radicals $CH_3C(O)OCHOO•CH_2OC(O)CH_3$, via reactions 11a and 12. The yield of $CH_3C(O)OC(O)CH_2OC(O)CH_3$ is independent of $O_2$ concentration, suggesting that reaction 15 is either very important or not very important for all $[O_2]$ studied, depending on the rate constant ratio, $k_{15}/k_{17}$. The fact that we observe significant amounts of $CH_3C(O)OC(O)H$ and $CH_3C(O)OH$ suggests that reaction 15 is not very important. The independence of the $CH_3C(O)OC(O)CH_2OC(O)CH_3$ yields on $[O_2]$ is consistent with the molecular channel of the self-reaction, reaction 14, being responsible for the anhydride formation. The molecular channel of the self-reaction of $CH_3C(O)OCHOO•CH_2OC(O)CH_3$ radicals, reaction 14, produces an alcohol, $CH_3C(O)OCHOHCH_2OC(O)CH_3$, along with acetoxyacetic acetic anhydride. While there are residual features in the product spectrum when the IR features of the identified products are subtracted, there are no features that are characteristic of an alcohol, such as an OH feature at 3600−3800 $cm^{-1}$. It is possible that this feature is weak; however, it is also possible that the alcohol is reactive and is quickly consumed by reaction with Cl atoms. The remaining $CH_3C(O)OCHOO•CH_2OC(O)CH_3$ radicals react with $RO_2$ to give alkoxy radicals, $CH_3C(O)OCHO•CH_2OC(O)CH_3$. As seen in Figure 6, the yield of $CH_3C(O)OH$ is small at high $[O_2]$, suggesting that α-ester rearrangement of $CH_3C(O)OCHO•CH_2OC(O)CH_3$, reaction 16, is not very important. The alkoxy radical decomposes to form $CH_3C(O)OC(O)H$ and $•CH_2OC(O)CH_3$, reaction 17. The alkyl peroxy radical, $CH_3C(O)OCH_2OO•$, is formed via reaction 18. Of the $CH_3C(O)OCH_2OO•$ radicals formed, some will react to form $CH_3C(O)OC(O)H$ via channels that are independent of $O_2$ concentration, reactions 22 and 23, while the balance will react with $RO_2$ to form $CH_3C(O)OCH_2O•$ radicals, reaction 19. The fate of $CH_3C(O)OCH_2O•$ radicals is either reaction with $O_2$ or α-ester rearrangement, reactions 20 and 21.

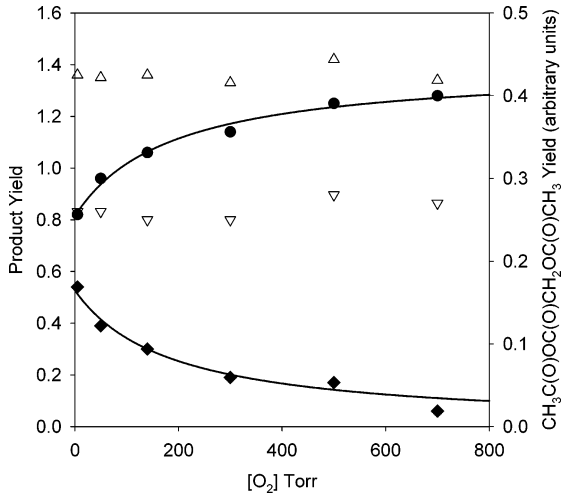


**Figure 6.** Yields of $CH_3C(O)OC(O)H$ (circles), $CH_3C(O)OH$ (diamonds), $CH_3C(O)OC(O)CH_2OC(O)CH_3$ (triangles down), and the combined yield of $CH_3C(O)OC(O)H$ and $CH_3C(O)OH$ (triangles up) versus the $O_2$ partial pressure following the UV irradiation of $CH_3C(O)O(CH_2)_2OC(O)CH_3/Cl_2/N_2/O_2$ mixtures at 700 Torr total pressure and 296 ± 1 K. Curves are the least-squares fits of expressions II and III to the data. See text for details.

$$2CH_3C(O)OCH_2OO• \rightarrow CH_3C(O)OC(O)H + CH_3C(O)OCH_2OH + O_2 \quad (22)$$

$$CH_3C(O)OCH_2OO• + HO_2• \rightarrow CH_3(O)OC(O)H + H_2O + O_2 \quad (23)$$

Christensen et al.[18] showed that, in the Cl atom initiated oxidation of methyl acetate, the dependence of the $CH_3C(O)OC(O)H$ and $CH_3C(O)OH$ yields on $[O_2]$ can be expressed in terms of the rate constant ratio $k_{20}/k_{21}$. The yields of $CH_3C(O)$-

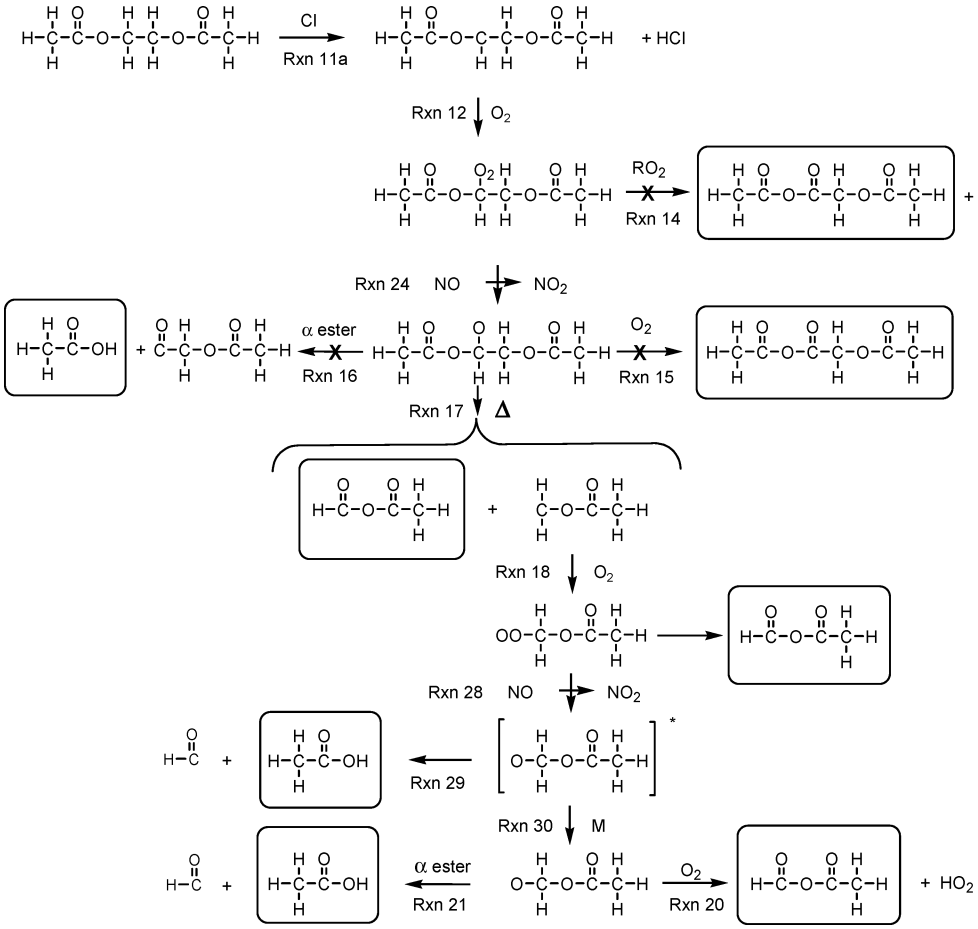


**Figure 7.** Diagram of the chlorine initiated oxidation of ethylene glycol diacetate in the presence of $NO_x$.

OC(O)H and $CH_3C(O)OH$ are given by

$$Y(CH_3C(O)OC(O)H) = \left[Y'(RO\bullet) \times \left(\frac{\frac{k_{20}}{k_{21}}[O_2]}{\frac{k_{20}}{k_{21}}[O_2]+1}\right)\right] + A \quad \text{(II)}$$

$$Y(CH_3C(O)OH) = \left[Y'(RO\bullet) \times \left(\frac{1}{\frac{k_{20}}{k_{21}}[O_2]+1}\right)\right] + B \quad \text{(III)}$$

where $Y'(RO\bullet)$ is the yield of the $CH_3C(O)OCH_2O\bullet$ radical. The terms $A$ and $B$ in the equations are required to account for the formation of $CH_3C(O)OC(O)H$ and $CH_3C(O)OH$ via channels that are independent of $O_2$ concentration. Christensen et al.[18] fit eqs II and III to their product data in the absence of NO and determined $k_{20}/k_{21} = 0.0054 \pm 0.0022$ Torr$^{-1}$. The curves in Figure 6 are least-squares fits of expressions II and III to the data using $k_{20}/k_{21} = 0.0054 \pm 0.0022$ Torr$^{-1}$. From the $CH_3C(O)OC(O)H$ data in Figure 6 we derive $Y'(RO\bullet) = 0.58 \pm 0.06$ and $A = 0.81 \pm 0.04$. From the $CH_3C(O)OH$ data in Figure 6 we derive $Y'(RO\bullet) = 0.53 \pm 0.10$ and $B = 0.03 \pm 0.03$. The values of $Y'(RO\bullet)$ derived from the $CH_3C(O)OC(O)H$ and $CH_3C(O)OH$ yields are consistent. Averaging the two determinations of $Y'(RO\bullet)$ together with uncertainties that encompass the individual measurements gives $Y'(RO\bullet) = 0.55 \pm 0.12$. The yield of $CH_3C(O)OH$ from $O_2$ independent channels is effectively zero. These parameters can be used to determine the yield of the $CH_3C(O)OCHO\bullet CH_2OC(O)CH_3$ radicals, $Y(RO\bullet)$, in the absence of NO. If decomposition is the sole fate of $CH_3C(O)OCHO\bullet CH_2OC(O)CH_3$ radicals and $\beta$ is the fraction of $CH_3C(O)OCH_2OO\bullet$ radicals that react to form $CH_3C(O)OC(O)H$ via channels that are independent of $O_2$ concentration, then the following equations apply.

$$Y(RO\bullet) + (\beta \times Y(RO\bullet)) = 0.81 \pm 0.04 \quad \text{(IV)}$$

$$Y(RO\bullet) - (\beta \times Y(RO\bullet)) = 0.55 \pm 0.12 \quad \text{(V)}$$

Solving these equations gives $Y(RO\bullet) = 0.68 \pm 0.06$ and $\beta = 0.19 \pm 0.11$. As discussed previously, the acetoxyacetic acetic anhydride reference spectrum used in this work is uncalibrated; however, the results presented here, together with carbon balance considerations, suggest that $Y(CH_3C(O)OC(O)CH_2OC(O)CH_3) \leq 0.16$ and $Y(CH_3C(O)OCHOHCH_2OC(O)CH_3) \leq 0.16$ due to the molecular channel of the $CH_3C(O)OCHOO\bullet CH_2OC(O)CH_3$ radical self-reaction, reaction 14. In this mechanistic analysis we have assumed no contribution from the attack of Cl atoms on the terminal $-CH_3$ groups. If attack occurs on the terminal $-CH_3$ groups, it is conceivable that a series of oxidations, followed by decomposition, would lead to formation of the $\bullet CH_2OC(O)CH_3$ radical. However, if this channel was significant, the values of $Y'(RO\bullet)$ derived from fits of eqs II and III would not be in agreement.

Mauer et al. [21] investigated the Cl atom initiated oxidation of ethylene glycol diformate, $HC(O)O(CH_2)_2OC(O)H$, in the absence of $NO_x$. They found that the alkoxy radical, $HC(O)OCHO(\bullet)CH_2OC(O)H$, decomposes to form formic acid anhydride, $HC(O)OC(O)H$, and $\bullet CH_2OC(O)H$. The fate of $\bullet CH_2$-

OC(O)H is a competition between reaction with $O_2$ to form HC(O)OC(O)H and α-ester rearrangement to form HC(O)OH and HC(O). In the absence of $NO_x$, the formic acid anhydride and formic acid yields were 144 ± 29 mol % and 39 ± 8 mol %, respectively.

**3.5. Products of the Cl Atom Initiated Oxidation of $CH_3C(O)O(CH_2)_2OC(O)CH_3$ in the Presence of NO.** The Cl atom initiated oxidation of ethylene glycol diacetate in the presence of NO was investigated by irradiating mixtures containing 3.3−7.0 mTorr $CH_3C(O)O(CH_2)_2OC(O)CH_3$, 24−26 mTorr NO, and 88−100 mTorr $Cl_2$. The experiments were performed at a constant total pressure of 700 Torr $O_2/N_2$ diluent with the $O_2$ partial pressure varied over the range 50−650 Torr. Reaction mixtures were subjected to 4−12 successive irradiations of 5−120 s duration. A diagram of the reaction pathways for the Cl atom initiated oxidation of ethylene glycol diacetate in the presence of $NO_x$ is given in Figure 7. In the presence of NO, $CH_3C(O)OCHO•CH_2OC(O)CH_3$ radicals are formed by reactions 11a and 12, followed by reaction 24.

$$CH_3C(O)OCHOO•CH_2OC(O)CH_3 + NO \rightarrow CH_3C(O)OCHO•CH_2OC(O)CH_3 + NO_2 \quad (24)$$

In the presence of $NO_x$, nitrites and nitrates may be formed through the following reactions

$$CH_3C(O)OCHOO•CH_2OC(O)CH_3 + NO \rightarrow CH_3C(O)OCH(ONO_2)CH_2OC(O)CH_3 \quad (25)$$

$$CH_3C(O)OCHO•CH_2OC(O)CH_3 + NO \rightarrow CH_3C(O)OCH(ONO)CH_2OC(O)CH_3 \quad (26)$$

$$CH_3C(O)OCHO•CH_2OC(O)CH_3 + NO_2 \rightarrow CH_3C(O)OCH(ONO_2)CH_2OC(O)CH_3 \quad (27)$$

Consistent with the fact that the reactions of oxygenated peroxy radicals with NO generally produce rather small yields of organic nitrates, there was no evidence in the IR spectra for the formation of nitrates. The formation of nitrites and nitrates via reactions 26 and 27 in the present experiments was suppressed by keeping $[NO]/[O_2] < 5 \times 10^{-4}$. In all experiments $CH_3C(O)OC(O)H$ and $CH_3C(O)OH$ were identified and quantified using calibrated reference spectra. Figure 8 shows the observed yields of the products versus the $O_2$ concentration. The presence of NO is expected to suppress the self-reaction of $CH_3C(O)OCHOO•CH_2OC(O)CH_3$ radicals, and, in fact, formation of $CH_3C(O)OC(O)CH_2OC(O)CH_3$ was not observed. As in the absence of NO, the yield of $CH_3C(O)OC(O)H$ increased with increasing $O_2$ concentration, while the yield of $CH_3C(O)OH$ decreased.

As discussed in the previous section, $CH_3C(O)OCHO•CH_2OC(O)CH_3$ radicals formed in reaction 24 will decompose via C−C bond cleavage

$$CH_3C(O)OCHO•CH_2OC(O)CH_3 \rightarrow CH_3C(O)OC(O)H + •CH_2OC(O)CH_3 \quad (17)$$

The $•CH_2OC(O)CH_3$ radicals will add $O_2$ to give the corresponding peroxy radicals.

$$CH_3C(O)OC•H_2 + O_2 \rightarrow CH_3C(O)OCH_2OO• \quad (18)$$

Christensen et al.[18] observed that the reaction of $CH_3C(O)OCH_2OO•$ with NO, reaction 28, produces excited alkoxy radicals, $CH_3C(O)OCH_2O•^*$, which either decompose via reaction 29 or lose their excess internal energy through collision with a third body, reaction 30. The thermalized $CH_3C(O)OCH_2O•$ radicals formed in reaction 30 either react with $O_2$, reaction 20, or undergo α-ester rearrangement, reaction 21.

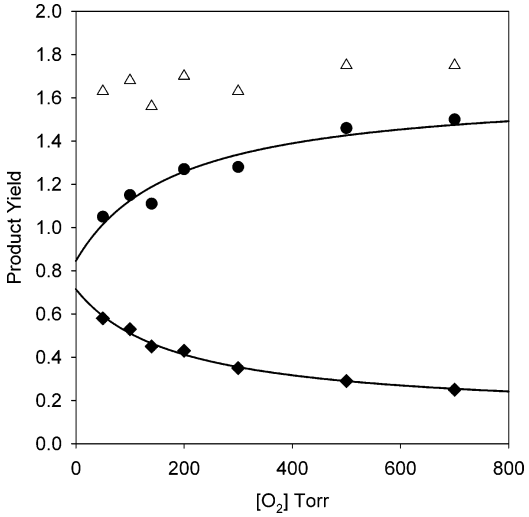


**Figure 8.** Yields of $CH_3C(O)OC(O)H$ (circles), $CH_3C(O)OH$ (diamonds), and the combined yield of $CH_3C(O)OC(O)H$ and $CH_3C(O)OH$ (triangles) versus the $O_2$ partial pressure following the UV irradiation of $NO/CH_3C(O)O(CH_2)_2OC(O)CH_3/Cl_2/N_2/O_2$ mixtures at 700 Torr total pressure and 296 ± 1 K. Curves are the least-squares fits of expressions II and III to the data. See text for details.

$$CH_3C(O)OCH_2OO• + NO \rightarrow CH_3C(O)OCH_2O•^* + NO_2 \quad (28)$$

$$CH_3C(O)OCH_2O•^* \rightarrow CH_3C(O)OH + HCO \quad (29)$$

$$CH_3C(O)OCH_2O•^* + M \rightarrow CH_3C(O)OCH_2O• + M \quad (30)$$

$$CH_3C(O)OCH_2O• + O_2 \rightarrow CH_3C(O)OC(O)H + HO_2• \quad (20)$$

$$CH_3C(O)OCH_2O• \rightarrow CH_3C(O)OH + HCO• \quad (21)$$

The curves in Figure 8 are least-squares fits of expressions II and III to the data using $k_{20}/k_{21} = 0.0054 \pm 0.0022$ Torr$^{-1}$. From the $CH_3C(O)OC(O)H$ data in Figure 8 we derive $Y'(RO•) = 0.80 \pm 0.20$ and $A = 0.84 \pm 0.11$. From the $CH_3C(O)OH$ data in Figure 8 we derive $Y'(RO•) = 0.58 \pm 0.06$ and $B = 0.13 \pm 0.03$. Averaging the two determinations of $Y'(RO•)$ together with uncertainties that encompass the individual measurements, $Y'(RO•) = 0.69 \pm 0.30$. These parameters can be used to determine the yield of $CH_3C(O)OCHO•CH_2OC(O)CH_3$ radicals, $Y(RO•)$, in the presence of NO. If decomposition is the sole fate of $CH_3C(O)OCHO•CH_2OC(O)CH_3$ radicals, $\beta$ is the fraction of $CH_3C(O)OCH_2OO•$ radicals that react to form $CH_3C(O)OC(O)H$ via channels that are independent of $O_2$ concentration and $\gamma$ is the fraction of $CH_3C(O)OCH_2O•$ radicals that undergo prompt α-ester rearrangement, then the following equations apply

$$Y(RO•) + (\beta \times Y(RO•)) = 0.84 \pm 0.11 \quad (VI)$$

$$Y(RO•) - (\beta \times Y(RO•)) - (\gamma \times Y(RO•)) = 0.69 \pm 0.30 \quad (VII)$$

$$\gamma \times Y(\mathrm{RO}\bullet) = 0.13 \pm 0.03 \qquad \text{(VIII)}$$

Solving these equations gives $Y(\mathrm{RO}\bullet) = 0.83 \pm 0.16$, $\beta = 0.02 \pm 0.02$, and $\gamma = 0.16 \pm 0.05$. Christensen et al.[18] determined that, in the presence of NO, the fraction of $CH_3C(O)OCH_2\bullet$ radicals which react to form $CH_3C(O)OC(O)H$ via processes that are not dependent on the $O_2$ concentration was $0.04 \pm 0.04$ and that the yield of alkoxy radicals which undergo prompt rearrangement to form $CH_3C(O)OH$ is $0.20 \pm 0.08$. The fit of the curves to the data in Figure 8 demonstrate that the fate of the $CH_3C(O)OCH_2O\bullet$ radical formed during the Cl initiated oxidation of ethylene glycol diacetate in the presence of NO is consistent with the fate of the $CH_3C(O)OCH_2O\bullet$ radical determined by Christensen et al.[18] in the Cl initiated oxidation of methyl acetate in the presence of NO.

Mauer et al.[21] investigated the Cl atom initiated oxidation of ethylene glycol diformate, $HC(O)O(CH_2)_2OC(O)H$, in the presence of $NO_x$. They found that the alkoxy radical, $HC(O)OCHO(\bullet)CH_2OC(O)H$, decomposes to form formic acid anhydride, $HC(O)OC(O)H$ and $\bullet CH_2OC(O)H$. The fate of $\bullet CH_2OC(O)H$ is reaction with $O_2$ to form $HC(O)OC(O)H$ and α-ester rearrangement to form $HC(O)OH$ and $HC\bullet(O)$. In the presence of $NO_x$, the molar yields of formic acid anhydride and formic acid were $173 \pm 34\%$ and $45 \pm 9\%$, respectively. Evidence was also found for a chemically activated alkoxy radical effect.

**4. Implications for Atmospheric Chemistry.** The present work improves our understanding of the atmospheric chemistry of ethylene glycol diacetate, $CH_3C(O)O(CH_2)_2OC(O)CH_3$. Cl atoms and OH radicals react with $CH_3C(O)O(CH_2)_2OC(O)CH_3$ with rate constants of $(5.7 \pm 1.1) \times 10^{-12}$ and $(2.36 \pm 0.34) \times 10^{-12}$ cm$^3$ molecule$^{-1}$ s$^{-1}$, respectively. The value of $k(\mathrm{OH} + CH_3C(O)O(CH_2)_2OC(O)CH_3)$ can be used to provide an estimate of the atmospheric lifetime of $CH_3C(O)O(CH_2)_2OC(O)CH_3$. Using a global weighted-average OH concentration of $1.0 \times 10^6$ molecules cm$^{-3}$ [22] leads to an estimated lifetime of $CH_3C(O)O(CH_2)_2OC(O)CH_3$ with respect to reaction with OH radicals of 4.9 days. The approximate nature of this atmospheric lifetime estimate should be stressed; the average daily concentration of OH radicals in the atmosphere varies significantly with both location and season. The value above is an estimate of the global average lifetime; local lifetime may be different. The major atmospheric oxidation products of ethylene glycol diacetate ($CH_3C(O)OC(O)CH_2OC(O)CH_3$, $CH_3C(O)OC(O)H$, and $CH_3C(O)OH$) are oxygenated organic compounds which are expected to be relatively unreactive toward further gas-phase oxidation reactions.[23] We conclude that ethylene glycol diacetate has a modest kinetic reactivity and a low mechanistic reactivity and appears likely to have a low photochemical ozone creation potential.

Modeling studies are required to provide a precise quantification of the photochemical ozone creation potential but are beyond the scope of the present work.

**Acknowledgment.** O.J.N. acknowledges financial support from the Danish Natural Science Research Council for the Copenhagen Center for Atmospheric Research (CCAR).

## References and Notes

(1) Meher, L. C.; Vidya Sagar, D.; Naik, S. N. *Renewable Sustainable Energy Rev.* **2006**, *10*, 248.
(2) *Biodiesel Handling and Use Guide*; U.S. Dept. of Energy DOE: GO-102006-2358; 2006.
(3) Ragauskas, A. J.; Williams, C. K.; Davison, B. H.; Britovsek, G.; Cairney, J.; Eckert, C. A.; Frederick, Jr., W. J.; Hallett, J. P.; Leak, D. J.; Liotta, C. L.; Mielenz, J. R.; Murphy, R.; Templer, R.; Tschaplinski, T. *Science* **2006**, *311*, 484.
(4) Atkinson, R. *J. Phys. Chem. Ref. Data* **1989**, Monograph 1.
(5) Sokolov, O.; Hurley, M. D.; Ball, J. C.; Wallington, T. J.; Nelsen, W.; Barnes, I.; Becker, K. H. *Int. J. Chem. Kinet.* **1999**, *31*, 357.
(6) Schijf, R.; Stevens, W. *Recl. Trav. Chim. Pays-Bas*. **1966**, *85*, 627.
(7) Sander, S. P.; Friedl, R. R.; Golden, D. M.; Kurylo, M. J.; Huie, R. E.; Orkin, V. L.; Moortgat, G. K.; Ravishankara, A. R.; Kolb, C. E.; Molina, M. J.; Finlayson-Pitts, B. J. *JPL Publ. 02-25*; Pasadena, CA, 2003.
(8) Wine, P. H.; Semmes, D. H. *J. Phys. Chem.* **1983**, *87*, 3572.
(9) Calvert, J. G.; Atkinson, R.; Kerr, J. A.; Madronich, S.; Moortgat, G. K.; Wallington, T. J.; Yarwood, G. *The mechanisms of atmospheric oxidation of the alkenes*; Oxford University Press: New York, 2000.
(10) Sørensen, M.; Kaiser, E. W.; Hurley, M. D.; Wallington, T. J.; Nielsen, O. J. *Int. J. Chem. Kinet.* **2003**, *35*, 191.
(11) O'Donnell, S. M.; Sidebottom, H. W.; Wenger, J. C.; Mellouki, A.; Le Bras, G. *J. Phys. Chem. A* **2004**, *108*, 7386.
(12) Atkinson, R. *Chem. Rev.* **1986**, *86*, 69.
(13) Kwok, E. S. C.; Atkinson, R. *Atmos. Environ.* **1995**, *29*, 1685.
(14) Atkinson, R. *Int. J. Chem. Kinet.* **1987**, *19*, 799.
(15) Mellouki, A.; Le Bras, G.; Sidebottom, H. *Chem. Rev.* **2003**, *103*, 5077.
(16) Notario, A.; Le Bras, G.; Mellouki, A. J. *Phys. Chem. A* **1998**, *102*, 3112.
(17) Tuazon, E. C.; Aschmann, S. M.; Atkinson, R.; Carter, W. P. L. *J. Phys. Chem. A* **1998**, *102*, 2316.
(18) Christensen, L. K.; Ball, J. C.; Wallington, T. J. *J. Phys. Chem. A* **2000**, *104*, 345.
(19) Picquet-Varrault, B.; Doussin, J. F.; Durand-Jolibois, R.; Carlier, P. *Phys. Chem. Chem. Phys.* **2001**, *3*, 2595.
(20) Picquet-Varrault, B.; Doussin, J. F.; Durand-Jolibois, R.; Carlier, P. *J. Chem. Phys.* **2002**, *106*, 2895.
(21) Mauer, T.; Hass, H.; Barnes, I.; Becker, K. H. *J. Phys. Chem. A* **1999**, *103*, 5032.
(22) Prinn, R. G.; Huang, J.; Weiss, R. F.; Cunnold, D. M.; Fraser, P. J.; Simmonds, P. G.; McCulloch, A.; Harth, C.; Salameh, P.; O'Doherty, S.; Wang, R. H. J.; Porter, L.; Miller, B R. *Science* **2001**, *292*, 1882.
(23) Derwent, R. G.; Jenkin, M. E.; Saunders, S. M. *Atmos. Environ.* **1996**, *30*, 181.